1521-0103/12/3432-342–350$25.00
THE JOURNAL OF PHARMACOLOGY AND EXPERIMENTAL THERAPEUTICS
Vol. 343, No. 2
197756/3801036

JPET 343:342–350, 2012

Target Binding Properties and Cellular Activity of Afatinib (BIBW 2992), an Irreversible ErbB Family Blocker[S]

Flavio Solca, Goeran Dahl,[1] Andreas Zoephel, Gerd Bader, Michael Sanderson, Christian Klein, Oliver Kraemer, Frank Himmelsbach, Eric Haaksma, and Guenther R. Adolf

Boehringer Ingelheim RCV GmbH & Co. KG., Vienna, Austria (F.S., G.D., A.Z., G.B., M.S., C.K., O.K., E.H., G.R.A.); and Boehringer Ingelheim Pharma GmbH & Co. KG., Biberach/Riss, Germany (F.H.)

Received June 25, 2012; accepted August 9, 2012

ABSTRACT

Deregulation of the ErbB (proto-oncogene B of the avian erythroblastosis virus AEV-H strain) receptor network is well recognized as an oncogenic driver in epithelial cancers. Several targeted drugs have been developed, including antibodies and small-molecule kinase inhibitors, each of them characterized by distinct patterns of ErbB receptor interactions. Understanding the precise pharmacological properties of these compounds is important for optimal use in clinical practice. Afatinib [BIBW 2992; *N*-[4-[(3-chloro-4-fluorophenyl)amino]-7-[[(3*S*)-tetrahydro-3-furanyl]oxy]-6-quinazolinyl]-4-(dimethylamino)-2-butenamide] is an ATP-competitive anilinoquinazoline derivative harboring a reactive acrylamide group. It was designed to covalently bind and irreversibly block enzymatically active ErbB receptor family members. Here, we show by X-ray crystallography the covalent binding of afatinib to wild-type epidermal growth factor receptor (EGFR) and by mass spectrometry the covalent interaction with EGFR, $EGFR^{L858R/T790M}$, human epidermal growth factor receptor 2 (HER2), and ErbB-4. Afatinib potently inhibits the enymatic activity of ErbB-4 (EC_{50} = 1 nM) and the proliferation of cancer cell lines driven by multiple ErbB receptor aberrations at concentrations below 100 nM. *N*-[4-[(3-chloro-4-fluorophenyl)amino]-7-[[(3*S*)-tetrahydro-3-furanyl]oxy]-6-quinazolinyl]-4-(dimethylamino)-2-butanamide (BI 37781), a close analog of afatinib lacking the acrylamide group and thus incapable of covalent bond formation, had similar potency on cells driven by EGFR or $EGFR^{L858R}$ but less or no detectable activity on cells expressing $EGFR^{L858R/T790M}$ HER2 or ErbB-4. These results stress the importance of the acrylamide group and show that afatinib differs from approved ErbB targeting agents by irreversibly inhibiting the kinase activity of all ErbB family members. They provide a mechanistic rationale for the distinct pharmacological features of this compound and explain the clinical activity seen in some patients who are resistant to antibody or kinase inhibitor therapy because of secondary mutations or ErbB receptor "reprogramming."

Introduction

The ErbB (proto-oncogene B of the avian erythroblastosis virus AEV-H strain) signaling network plays a central role in epithelial tissue development and homeostasis. At least 10 different ligands regulate the activity of ErbB receptors, which signal as ligand-induced dimers formed by four related transmembrane receptor tyrosine kinases, EGFR/ErbB-1/HER1, HER2/ErbB-2/neu, HER3/ErbB-3, and HER4/ErbB-4. In the absence of ligand, the extracellular domains of EGFR, ErbB-3, and ErbB-4 adopt an autoinhibited conformation. Ligand binding triggers a conformational change in the extracellular domain, and masked dimerization residues become exposed at the protein surface, thus allowing homodimerization and/or heterodimerization. HER2 differs from other family members because it lacks a reported ligand and its extracellular domain is permanently poised in an "active-like" conformation (Graus-Porta et al., 1997; Garrett et al., 2003). Although controversially discussed (Alvarado et al., 2009), it has been proposed that HER2 is the preferred heterodimerization partner for other family members (Graus-Porta et al., 1997).

Receptor dimerization results in the formation of asymmetrical (tail-to-head) complexes of the partnered catalytic domains. In such dimers, one monomer acts as an allosteric

The work was supported entirely by Boehringer-Ingelheim.
[1]Current affiliation: AstraZeneca R&D, Mölndal, Sweden.
Article, publication date, and citation information can be found at http://jpet.aspetjournals.org.
http://dx.doi.org/10.1124/jpet.112.197756.
[S] The online version of this article (available at http://jpet.aspetjournals.org) contains supplemental material.

ABBREVIATIONS: EGF, epidermal growth factor; EGFR, EGF receptor; HER, human EGFR; WT, wild type; GST, glutathione transferase; KD, kinase domain; PBS, phosphate-buffered saline; SPR, surface plasmon resonance; DTT, dithiothreitol; MS, mass spectrometry; MS/MS, tandem MS; BIBW 2992, *N*-[4-[(3-chloro-4-fluorophenyl)amino]-7-[[(3*S*)-tetrahydro-3-furanyl]oxy]-6-quinazolinyl]-4-(dimethylamino)-2-butenamide; BI 37781, *N*-[4-[(3-chloro-4-fluorophenyl)amino]-7-[[(3*S*)-tetrahydro-3-furanyl]oxy]-6-quinazolinyl]-4-(dimethylamino)-2-butanamide.

activator and induces activation of the intrinsic catalytic activity of the partnered receptor (Zhang et al., 2006). Specific tyrosine residues within the C-terminal regulatory domain of the activating partner become transphosphorylated and subsequently act as docking sites for adaptor proteins, which engage multiple signaling pathways including the rat sarcoma/rapidly accelerated fibrosarcoma/mitogen-activated protein kinase, the phosphoinositide 3-kinase/AKT/ mammalian target of rapamycin, the Janus kinase/signal transducer and activator of transcription, and the phospholipase Cγ/ protein kinase C cascades. The exact nature of the intracellular signal depends on the signaling context, the particular ErbB dimers formed, and the expression of ErbB receptors and their ligands (Tzahar et al., 1996).

Aberrant signaling through the ErbB growth factor receptor system is found in many types of epithelial cancers (Yarden and Sliwkowski, 2001; Zhang et al., 2007). Receptor mutations and/or gene amplifications as well as overproduction of particular ligands are among the best-described oncogenic mechanisms. EGFR mutations that disrupt the inactive extracellular conformation (e.g., EGFR variant type III) or induce/stabilize the active form of the intracellular catalytic domain (e.g., L858R point mutation or exon 19 deletions) have been identified and validated as cancer-promoting mechanisms (Lynch et al., 2004; Ji et al., 2006). Likewise, HER2 gene amplification has been observed in breast and gastric cancer, and ErbB4 mutations have been described in tumor samples from patients with non–small-cell lung cancer, melanoma, and breast and colon cancer (Slamon et al., 1987; Prickett et al., 2009; Bang et al., 2010).

The increased understanding of the role of ErbB receptor deregulation in cancer promotion triggered the development of a number of therapeutic agents. The armamentarium of approved ErbB-directed drugs includes specific antibodies that prevent ligand binding and/or receptor dimerization (e.g., cetuximab targeting EGFR, trastuzumab specific for HER2) and molecules targeting the intrinsic catalytic activity of ErbB receptors (e.g., gefitinib, erlotinib, or lapatinib). Additional inhibitors are currently in clinical development. These low-molecular-weight compounds generally bind to the ATP pocket of the enzymes, but show remarkable diversity in their potency for the inhibition of different ErbB family members and EGFR mutant isoforms. Although some inhibitors bind reversibly to either the inactive or the active conformation of the kinase domains, others contain a reactive chemical group potentially allowing the formation of a covalent bond to the active site of the target (Eck and Yun, 2010).

Understanding the selectivity and binding mode of an ErbB-directed small molecule is an important prerequisite for its optimal use in the clinical setting. In contrast to currently approved ErbB kinase inhibitors with reversible binding mode (i.e., erlotinib, gefitinib, and lapatinib), afatinib [BIBW 2992; *N*-[4-[(3-chloro-4-fluorophenyl)amino]-7-[[(3*S*)-tetrahydro-3-furanyl]oxy]-6-quinazolinyl]-4-(dimethylamino)-2-butenamide], which is currently being assessed in clinical phase III trials in patients with lung, breast, and head and neck cancer (Li et al., 2008; www.clinicaltrials.gov) contains an electrophilic group capable of Michael addition to conserved cysteine residues within the catalytic domains of EGFR (Cys797), HER2 (Cys805), and ErbB-4 (Cys803). Here, we show for the first time that afatinib covalently binds to its targets and irreversibly inhibits their enzymatic activity, which results in the inhibition of ErbB-4 and long-lasting cellular activity.

Materials and Methods

Cell Culture and Reagents. All cells were obtained from the American Type Culture Collection (Manassas, VA) and cultured according to the provider's instructions. Master stocks have been generated and authenticated by single-nucleotide polymorphism chip analysis by using the Sanger Institute databases (http://www.sanger.ac.uk/resources/databases/) as reference. ErbB kinase domains 0102-0000-1 (EGFR), 0724-0000-1 ($EGFR^{T790M}$), 0725-0000-1 ($EGFR^{T790M/L858R}$), 0108-0000-1 (ErbB2), and 0109-0000-1 (ErbB4) were obtained as expressed glutathione transferase (GST)-fusion proteins in Sf9 cells (ProQinase, GmbH, Freiburg, Germany).

Surface Plasmon Resonance Evaluation. Surface plasmon resonance (SPR) monitoring mass density changes was used to measure drug-target interactions. All SPR experiments were performed at Beactica AB (Uppsala, Sweden) on a Biacore T100 instrument (Biacore AB, Uppsala, Sweden). GST-His6-tagged kinase domains (His672-Ala1210) of EGFR for wild type ($EGFR^{WT}$) and the L858R/T790M variant (ProQinase) were injected over a CM3 sensor chip (Biacore AB), coated with anti-His6 antibodies (GE Healthcare, Chalfont St. Giles, Buckinghamshire, UK), using 25 mM Hank's balanced salt solution (Sigma, St. Louis, MO), 0.05% Tween 20 (BHD/Prolado; VWR, West Chester, PA), pH 7.4 as running buffer. All interaction experiments were carried out at 25°C at a final dimethyl sulfoxide concentration of 5% (v/v) in running buffer at a flow rate of 30 μl/min. The pH of this running buffer was adjusted to pH 7.0 or 8.0 by using sodium hydroxide. Compounds were analyzed at 200 nm concentration by using 300-s contact time followed by 600-s dissociation time. All measurements were performed at least three times. Data were analyzed by using Biacore T100 software 2.0 or BIA evaluation software 4.1 (Biacore AB). Reference and blank subtracted data were corrected for baseline drift and normalized before data analysis. The interaction models were fitted to the data for each compound and protein surface separately. For $EGFR^{WT}$, up to 1000 response units of protein with high (70–100%) surface activity could be reached, whereas capture of the $EGFR^{L858R/T790M}$ variant resulted in lower surface activity (30–50%). None of the compounds tested were found to interact with the immobilized capture antibodies in the concentration range used (data not shown).

Protein Production for Crystallography and Data Analysis. Protein preparation and crystallographic work was done at Proteros Biostructures GmbH (Martinsried, Germany). The protein kinase domain of the human epidermal growth factor receptor (EGFR-KD; Gly696-Gly1022, numbering according to SwissProt entry P00533) was cloned in pFastBac 1 as a thrombin-cleavable GST fusion. Recombinant baculovirus was produced by using the Bac-to-Bac-system, and the protein was expressed by infection of Sf9 cells with high titer virus stock in 10L single-use bioreactors (Wave Biotech; GE Healthcare). Cells were controlled for infection and viability, harvested 48 to 64 h after infection, and stored at −80°C until purification. For purification, cells were thawed in 40 ml of lysis buffer (1× PBS supplemented with 10% glycerol, 5 mM ß-mercaptoethanol, and protease inhibitor tabs) per liter of culture medium and lysed by using an Ultra-Turrax device (IKA Works, Inc., Wilmington, NC). After centrifugation, the lysate was loaded onto a glutathione Sepharose column (GE Healthcare) equilibrated in lysis buffer without protease inhibitor, and bound protein was eluted by using 20 mM Tris/Cl, pH 8.0, 150 mM NaCl, 10% glycerol, 10 mM glutathione, and 5 mM dithiothreitol (DTT). The GST tag was removed by using thrombin (GE Healthcare), and EGFR-KD was separated from GST by a second passage over the same column. The flow-through of this column was pooled, and EGFR-KD was purified to >90% homogeneity as judged by SDS-polyacrylamide gel electrophoresis on a Super-

dex75 column (GE Healthcare) equilibrated in 50 mM Tris/Cl, pH 8.0, 500 mM NaCl, 10% glycerol, and 5 mM DTT. For crystallization, the protein was buffer-exchanged by using NAP25 columns (GE Healthcare).

The T790M-mutant was generated by using the QuikChange site-directed mutagenesis kit (Agilent Technologies, Santa Clara, CA), and the mutant protein was produced by following the protocols for the wild type.

Crystallization of wild-type EGFR-KD was performed similar to previously described procedures (Stamos et al., 2002). Before crystallization protein was concentrated to a final concentration of 12 mg/ml in 20 mM Tris, pH 8.0, 0.1 mM benzamidine, and 1 mM DTT. This buffer was also used for protein dilution before crystallization. The sample was filtrated before setup of drops (0.22 μm centrifugal filter units; Millipore Corporation, Billerica, MA). Crystals of wild-type EGFR-KD with benzamidine were produced by vapor diffusion setup. Drops were set as follows: 0.5 μl of protein (8 mg/ml, dilution buffer see above) was mixed with 0.5 μl of reservoir solution in hanging drops. The reservoir solution contained 1.4 M KNa-tartrate, 0.1 M HEPES, pH 7.0, and 2 mM DTT. Crystals appeared after 1-day incubation at 20°C. For soaking crystals were transferred to a solution containing 5 mM afatinib, 1.5 M KNa-tartrate, 0.1 M HEPES, pH 7, and 5% dimethyl sulfoxide. Crystals were soaked overnight by transfer to 25% glycerol in reservoir and direct freezing in liquid nitrogen.

For crystallization of the T790M mutant, before crystallization 1 μM afatinib was added to the protein before concentrating the protein to a final concentration of 8 mg/ml in the buffer containing 50 mM Tris, pH 8.0, 500 mM NaCl, 10% glycerin, and 5 mM tris(2-carboxyethyl) phosphine hydrochloride. Crystals of EGFR-KD were produced by vapor diffusion setup. Drops were set as follows: 0.5 μl of protein was mixed with 0.5 μl of reservoir solution in hanging drops. The reservoir solution contained 27% polyethylene glycol 6000, 0.3 M NaCl, 0.1 M HEPES, pH 8.0, and 5 mM tris(2-carboxyethyl) phosphine hydrochloride (Yun et al., 2008). Crystals appeared overnight at 20°C. The X-ray diffraction data were collected from cocrystals of EGFR or $EGFR^{T790M}$ with afatinib at the Swiss Light Source synchrotron facility (Villigen, Switzerland) under cryogenic conditions. Data were processed by using the XDS package (Kabsch, 2010). The phase information necessary to determine and analyze the structures was obtained by molecular replacement. A published model of EGFR (Protein Data Bank ID code 1M17) (Stamos et al., 2002) was used as a search model. Subsequent model building and refinement was performed according to standard protocols with the CCP4 (Collaborative Computational Project, Number 4, 1994) and COOT (Emsley et al., 2010) software packages. Statistics of the final structures and the refinement processes are listed in the Supplementary Material. The coordinates of EGFR and $EGFR^{T790M}$ complexed with afatinib as well as the respective structure factors have been deposited at the Protein Data Bank under accession codes 4G5J and 4G5P.

Mass Spectrometric Analyses. The recombinant enzymes EGFR, $EGFR^{T790M/L858R}$, HER2, and ErbB-4 (ProQinase) tagged with a GST-His tag were captured on a Ni-IMAC column (Ni-NTA Superflow; QIAGEN, Valencia, CA) and washed with 50 mM HEPES pH 7.5 buffer to remove glutathione and DTT. The immobilized proteins were incubated with a 10-fold (EGFR isoforms) to 20-fold molar excess of afatinib for 60 (EGFR isoforms) or 120 min at 37°C, and free afatinib was removed by washing before pepsin cleavage. Peptic peptides were collected from the supernatant after centrifugation, separated on a C18 column (Luna C18; Phenomenex, Torrance, CA), and collected for electrospray ionization-tandem mass spectrometry (MS/MS) analysis (Dionex Ultimate 3500 NCS; Thermo Fisher Scientific, Waltham, MA). Chemically synthesized peptides covalently modified with afatinib corresponding to the pepsin cleavage product were used as reference for high-performance liquid chromatography and electrospray ionization-MS/MS analyses.

Kinase Inhibition Assays. Nonradioactive in vitro kinase assays were performed as described previously (Solca et al., 2004; Li et al., 2008). The final ATP concentrations were adjusted individually to saturation (50 μM for EGFR and 250 μM for HER2). ErbB-4 kinase activity was determined in a radioactive kinase assay format (Solca et al., 2004; Li et al., 2008) at a final ATP concentration of 50 μM.

Transient Transfection Experiments. The full-length ErbB-4 receptor (transcript variant JM-a/CVT-1 with GenBank accession number NM_005235) was cloned into the pCMV6-XL4 vector (GenBank accession number AF067196) and used for transient transfection experiments in NIH-3T3 cells. Expression of ErbB-4 was time-dependent and maximal 48 h postinfection. Cellular assays were performed as described above. HER4 was detected by Western blot analyses from transfected cell extracts by using a rabbit monoclonal antibody HER4/ErbB4 clone 83B10 (Cell Signaling Technology, Danvers, MA).

Cellular EGFR and HER2 Phosphorylation Assays. The enzyme-linked immunosorbent assay methods used for assessing EGFR and HER2 phosphorylation in cellular models were reported previously (Solca et al., 2004; Li et al., 2008). In brief, 1×10^4 near-confluent A431 cells (American Type Culture Collection), NCI-H1975 cells (American Type Culture Collection), or 2×10^4 BT474/HTB-20 cells (American Type Culture Collection) were used for the enzyme-linked immunosorbent assay experiments. For phospho-EGFR determination serial dilutions of compounds were incubated for 1 h before EGF stimulation (Promega, Madison, WI; 100 ng/ml) for 10 min at room temperature. Cells were washed two times with ice-cold PBS before extraction as described previously (Li et al., 2008). To detect HER2 phosphorylation in BT474 cells ligand stimulation was not necessary, because these cells display constitutive HER2 phosphorylation under the culture conditions. Therefore, a 100-μl aliquot of 2× HEPES buffer was directly added to each well after the 1-h incubation period with compounds. Extractions were performed on a microtiter plate shaker for 1 h.

Cellular Proliferation Assays. The effect of ErbB inhibitors on cellular proliferation was tested in various assay formats including anchorage-dependent (BT474 cells grown on plastic; two-dimensional assays) and anchorage-independent (NCI-H1975 cells grown in soft agar; three-dimensional assays) assays. BT474 cells growing in Dulbecco's modified Eagle's medium (Lonza Walkersville, Inc., Walkersville, MD) were harvested, counted, and used for the fluorescence assay according to the method of Dengler et al. (1995). In brief, 2×10^4 cells were seeded in 90 μl of medium in each well of a 96-well flat-bottomed microtiter in the presence of serial dilutions of test compounds diluted in 10% dimethyl sulfoxide/PBS to a final assay concentration of 1%. The concentration of the test compounds covered a range between 50 μM and 0.8 nM. Each drug concentration was plated in duplicate. After 96 h of continuous drug exposure nonviable cells were stained by addition of 25 μl/well of a propidium iodide solution (50 μg/ml). The basal fluorescence (FU1) was measured after 10 min of incubation in the dark by using a Labsystems Fluoroskan II micro-plate reader (Global Medical Instrumentation, Inc., Ramsey, MN; excitation 544 nm; emission 612 nm). After measurement, the culture medium was removed, and cells were permeabilized by freezing the plates at −80°C for at least 90 min. After thawing, propidium iodide (100 μl/well of 12.5 μg/ml) was added to the plates, which were incubated for 10 min at room temperature in the dark. A second fluorescence measurement (FU2) was taken to estimate the amount of total cells. The number of viable cells was calculated as the difference between these two measurements (FU2-FU1). The data were analyzed by using the program Prism (GraphPad Software, Inc., San Diego, CA). The inhibitor concentrations were transformed to logarithmic values, and the raw data were normalized. The normalized values were used to calculate the EC_{50} by a nonlinear regression curve fit (sigmoidal dose-response; variable slope). NCI-H1975 cells (American Type Culture Collection) were grown in RPMI 1640 medium supplemented with 10% fetal calf

serum and prepared for three-dimensional assays (0.3% sea plaque agarose top layer) as described previously (Li et al., 2008).

Results

Biochemical and Biophysical Characterization of Kinase Inhibitor Interactions. The inhibitory profile of afatinib in biochemical EGFR and HER2 kinase assays has been reported previously (Li et al., 2008). Afatinib is a highly potent inhibitor of wild-type EGFR (EC_{50} = 0.5 nM) and HER2 (14 nM) and the oncogenic mutants $EGFR^{L858R}$ (0.4 nM) and $EGFR^{L858R/T790M}$ (10 nM), the latter is known to be associated with resistance to approved EGFR inhibitors like erlotinib. We have now expanded those observations to include assessments on ErbB-4 inhibitory activity and a comparison with structurally distinct ErbB kinase inhibitors. Furthermore, we have designed, synthesized, and profiled *N*-[4-[(3-chloro-4-fluorophenyl)amino]-7-[[(3*S*)-tetrahydro-3-furanyl]oxy]-6-quinazolinyl]-4-(dimethylamino)-2-butanamide (BI 37781), a compound with close structural similarity to afatinib that lacks the reactive double bond and thus is incapable of forming a covalent bond to the catalytic site cysteine residues (Fig. 1). The new biochemical data (Table 1) reveal that afatinib also potently inhibits the kinase activity of ErbB-4 with an EC_{50} of 1 nM. In comparison with afatinib, BI 37781, which showed similar potency on wild-type EGFR, was 5-fold less active on the L858R EGFR mutant, $EGFR^{L858R/T790M}$, HER2 and, most strikingly, ErbB-4 with a 500-fold loss (EC_{50} = 544 nM). For comparison (Table 1), we included additional EGFR inhibitors in our assays. Canertinib, a kinase inhibitor containing a reactive acrylamide group, showed a selectivity profile similar to afatinib, whereas the reversible inhibitors gefitinib and erlotinib, similar to BI 37781, potently inhibited only $EGFR^{WT}$ and $EGFR^{L858R}$. Compared with afatinib and canertinib, the reversible inhibitor lapatinib was 30-fold less potent on ErbB-4 and failed to inhibit $EGFR^{L858R/T790M}$ even at high concentrations.

We further characterized the binding properties of afatinib and BI 37781 by using SPR technology at physiological pH 7.0. Tight binding to the EGFR targets prohibited accurate determination of rate constants but allowed for qualitative interaction analyses. Various interaction models were tested and compared with the 1:1 model ($E + l \leftrightharpoons El$); of these, the induced-fit model was found to most accurately describe the complex interaction patterns observed (Fig. 2). In this model the inhibitor forms an initial weak complex with the protein (EI), which then transforms into a tighter complex (EI*) ($E + l \leftrightharpoons El \leftrightharpoons El^*$). The two EGFR variants differed mainly in the dissociation phases, with SPR sensorgrams showing a much slower dissociation from $EGFR^{WT}$ compared with $EGFR^{L858R/T790M}$ for both compounds. Afatinib dissociated more slowly from $EGFR^{L858R/T790M}$ compared with BI 37781 (Fig. 2A). The SPR data also shows that under the present experimental conditions afatinib did not completely saturate all binding sites on the biosurface. Further binding analyses were performed at pH 8.0, reasoning that the Cys797 in EGFR would act as a stronger nucleophile thus favoring covalent bond formation. In line with this hypothesis, slower dissociation was observed at pH 8.0 compared with pH 7.0 for afatinib on both protein variants, whereas BI 37781 displayed essentially identical interaction patterns at both pH values (Fig. 2B).

The crystal structure of the afatinib/EGFR kinase domain complex was solved at 2.8-Å resolution (R_{cryst} = 20.5%; R_{free} = 25.9%), revealing detailed binding interactions (Fig. 3). The protein showed bilobal architecture characteristic of the protein kinase superfamily (Fig. 3A), and structural results are in line with previously reported EGFR kinase domain data (Stamos et al., 2002). A rather long hydrogen bond (3.3 Å) was formed between the amide nitrogen of Met793 at the hinge region and the quinazoline core of the inhibitor

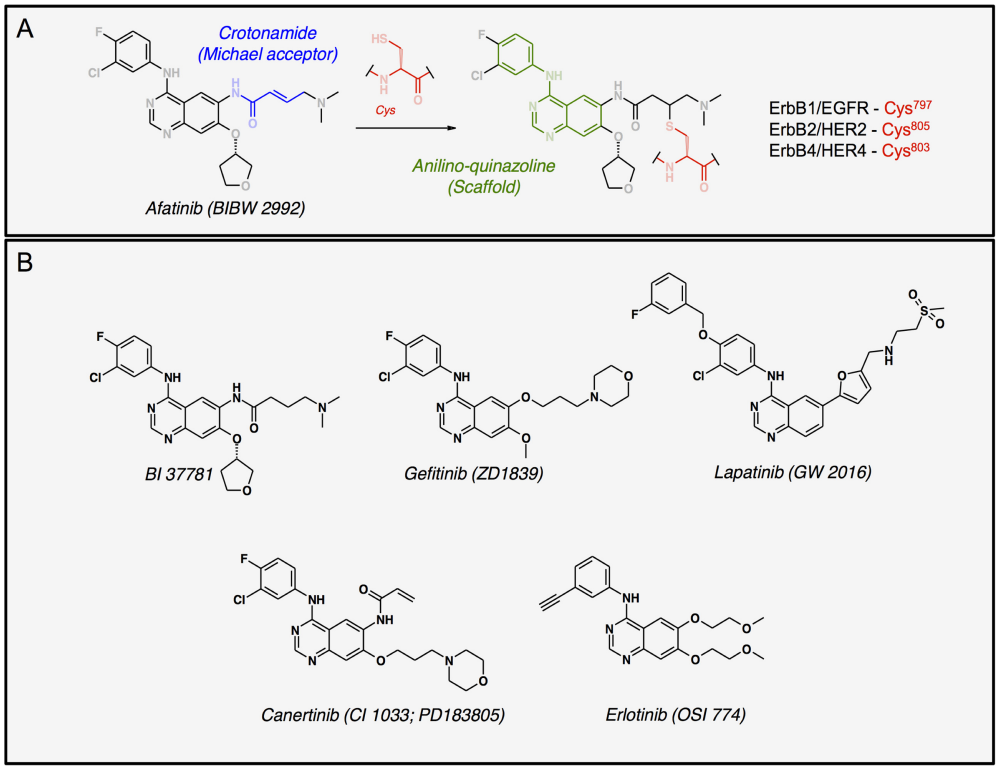

Fig. 1. Structures of chemical entities targeting ErbB receptor family members. A, the postulated covalent mode of binding of afatinib to a reactive cysteine. B, the structures of the small-molecule kinase inhibitors used in this study.

TABLE 1

Potency of ErbB receptor inhibitors in molecular and cellular assays

The inhibitory constants [nM] were determined as described under *Materials and Methods*. All values were derived from technical duplicates and confirmed in multiple (n) independent biological experiments. Values in bold were determined in the same experiment to allow direct comparison. The range of confirmatory values that comprise 197 independent EC_{50} determinations includes 16 EC_{50} values reported previously (Li et al., 2008) marked by *.

	Compounds					
	Afatinib	BI 37781	Lapatinib	Canertinib	Erlotinib	Gefinitib
ErbB-4 kinase						
Value	**1**	**544**	**30**	**1**	**579**	**323**
Range	0.7–1.7	510–544	18–30	0.8–10	579–756	293–323
n	4	2	3	4	2	2
$EGFR^{WT}$ kinase						
Value	**0.5**	**0.8**	—	—	—	—
Range	0.2–0.7	0.8–1	0.3–17	0.3*–1.7	0.9–1.7	0.4–4.7
n	5	2	6	5	4	6
$EGFR^{L858R}$ kinase						
Value	**0.2**	**1**	—	—	—	—
Range	0.2–0.4*	1–2	2–8*	0.4–0.8*	1.1–2.7	0.8–1.4
n	2	2	3	2	3	2
$EGFR^{L858R/T790M}$ kinase						
Value	**9**	**57**	—	—	—	—
Range	9–10*	36–57	>4000	18–36	1520–3562	534–1267
n	2	2	3	3	3	4
HER2 kinase						
Value	**14**	**84**	—	—	—	—
Range	7–25	84–112	6–25	22–72	238–698	416–1830
n	5	2	4	3	3	6
Phospho EGFR (A431), EGFR WT kinase						
Value	**8**	**17**	—	—	—	—
Range	8–13*	17–56	93–145	17–22*	3–8	22–63
n	4	2	4	5	5	4
Phospho EGFR (NCI-H1975), EGFR L858R/T790M						
Value	**49**	**1610**	—	—	—	—
Range	49–129	1458–1610	>4000*	76–88	>4000*	>4000*
n	5	2	2	3	3	3
Phospho HER2 (BT474), HER2 gene amplification						
Value	**75**	**570**	—	—	—	—
Range	35*–75	570–1237	74–102	88–184*	396–930	3600–3710*
n	5	3	3	2	3	2
Proliferation (NCI-H1975), L858R/T790M (three-dimensional assays)						
Value	**92**	**>3000**	—	—	—	—
Range	92–225	>3000	>4000*	57–307	>4000*	>4000*
n	4	2	2	4	3	3
Proliferation (BT474), HER2 gene amplification, two-dimensional assays.						
Value	**54**	**>4000**	—	—	—	—
Range	12–56	>4000	12–128	37–66	599–899	1070–1960
n	5	3	3	3	3	3

(Fig. 3B). Most important, in addition to the noncovalent interactions, the electron density clearly showed a covalent bond formed between Cys797 at the edge of the active site and the Michael-acceptor group of afatinib. During the refinement process, the bond length for the C-S link was restrained to 1.82 Å. As shown in Supplemental Fig. 3S1 the electron density unambiguously indicates the formation of the covalent C-S bond. The structure of the $EGFR^{T790M}$ mutant in complex with afatinib was also solved (Protein Data Bank ID code 4G5P); however, the electron density around the dimethylamine group of afatinib was of lower resolution but suggested the formation of a covalent bond to Cys797. For confirmation, alternative approaches to prove the covalent interaction with this EGFR mutant were performed.

For this purpose target-inhibitor complexes were analyzed by MS. The purified kinase domains of $EGFR^{WT}$, $EGFR^{L858R/T790M}$, HER2, and ErbB-4 were incubated with afatinib and digested with pepsin, and afatinib-peptide adducts were separated by liquid chromatography/MS). The MS/MS spectra for all four constructs showed a peak at 520.17 Da that could be assigned to afatinib (486.18 Da) containing a protonated sulfur atom (34 Da), which originated from the respective Cys797 of EGFR, Cys805 of HER2, or Cys803 of ErbB-4 residues. For further confirmation, we compared the spectra resulting from a synthetic reference peptide derived from $EGFR^{L858R/T790M}$ and the peptic peptide adduct obtained under experimental conditions. The data reported in Fig. 4 show that both spectra were essentially identical, confirming that afatinib covalently engages the $EGFR^{L858R/T790M}$ mutant at residue 797. Similar MS/MS spectra were generated by using the reference peptides for HER2 and ErbB-4, corroborating covalent modification at Cys805 and Cys803, respectively (see Supplemental Fig. 4, S1 and S2, respectively). The identification of ion peaks corresponding to afatinib plus a sulfur atom and corresponding peptide adducts in the MS/MS spectra of EGFR [wild type (data not shown) as well as T790M], HER2, and ErbB-4 (Fig. 4 and Supplemental Fig.

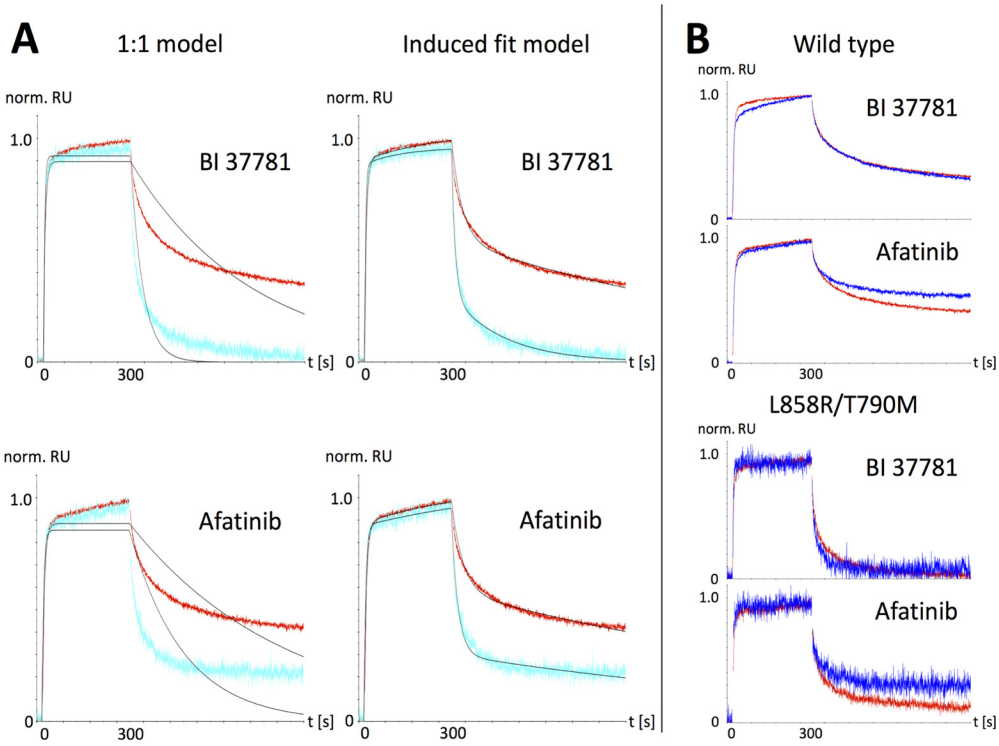

Fig. 2. Surface plasmon resonance sensorgrams show that afatinib binding follows an induced-fit mechanism. The *y* axis shows the normalized responses, and the *x* axis shows the elapsed time. The compounds were analyzed at a concentration of 200 nM with a contact time of 300 s followed by 600-s dissociation. A, fitting of the 1:1 model ($E + l \leftrightharpoons El$; left) or the induced-fit model ($E + l \leftrightharpoons El \leftrightharpoons El^*$; right) to sensorgrams obtained by using BI 37781 and afatinib on wild type (red) or L858R/T790M (cyan) variants of the EGFR kinase domain. The fitted interaction models are shown in black. B, interaction of BI 37781 and afatinib with wild type or L858R/T790M variants of EGFR kinase domain at pH 7.0 (red) or pH 8.0 (blue).

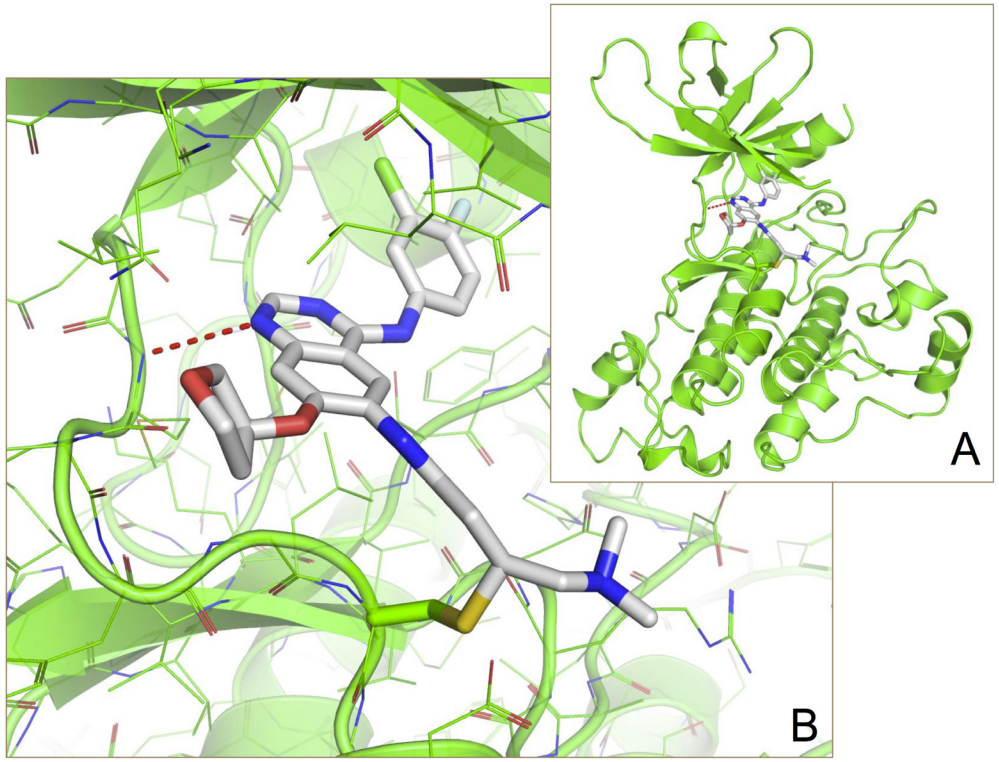

Fig. 3. Crystal structure of wild-type EGFR (residues Gly696-Gly1022) in complex with afatinib. A, the structure of the whole EGFR kinase domain. B, a close-up of the hinge region. The dotted line represents a 3.3-Å hydrogen bond formed between the amide nitrogen of Met793 at the hinge region and the quinazoline core of afatinib. Tables showing the statistics of data collection and processing as well as refinement statistics can be found in Supplemental Fig. 3S2.

4, S1 and S2) unequivocally demonstrates the ability of afatinib to form a covalent bond with all enzymatically active ErbB receptors. The observation that a peak representing an afatinib-cysteine adduct is lacking in both the experimental sample and the control peptide is best explained by the high fragmentation energy used in these experiments, a phenomenon that has been observed previously (Oberth and Jones, 1997; Sleno et al., 2007).

Cellular Activity of ErbB Inhibitors. The differences between afatinib and its close analog BI 37781 revealed by binding and enzymatic assays were more pronounced in cellular assays. Both compounds potently inhibited EGFR signaling (autophosphorylation assay in cancer cell lines expressing wild-type EGFR (A431, EC_{50} = 8 and 17 nM, respectively). Whereas afatinib also inhibited signaling in cell lines expressing mutant $EGFR^{L858R/T790M}$ (NCI-H1975,

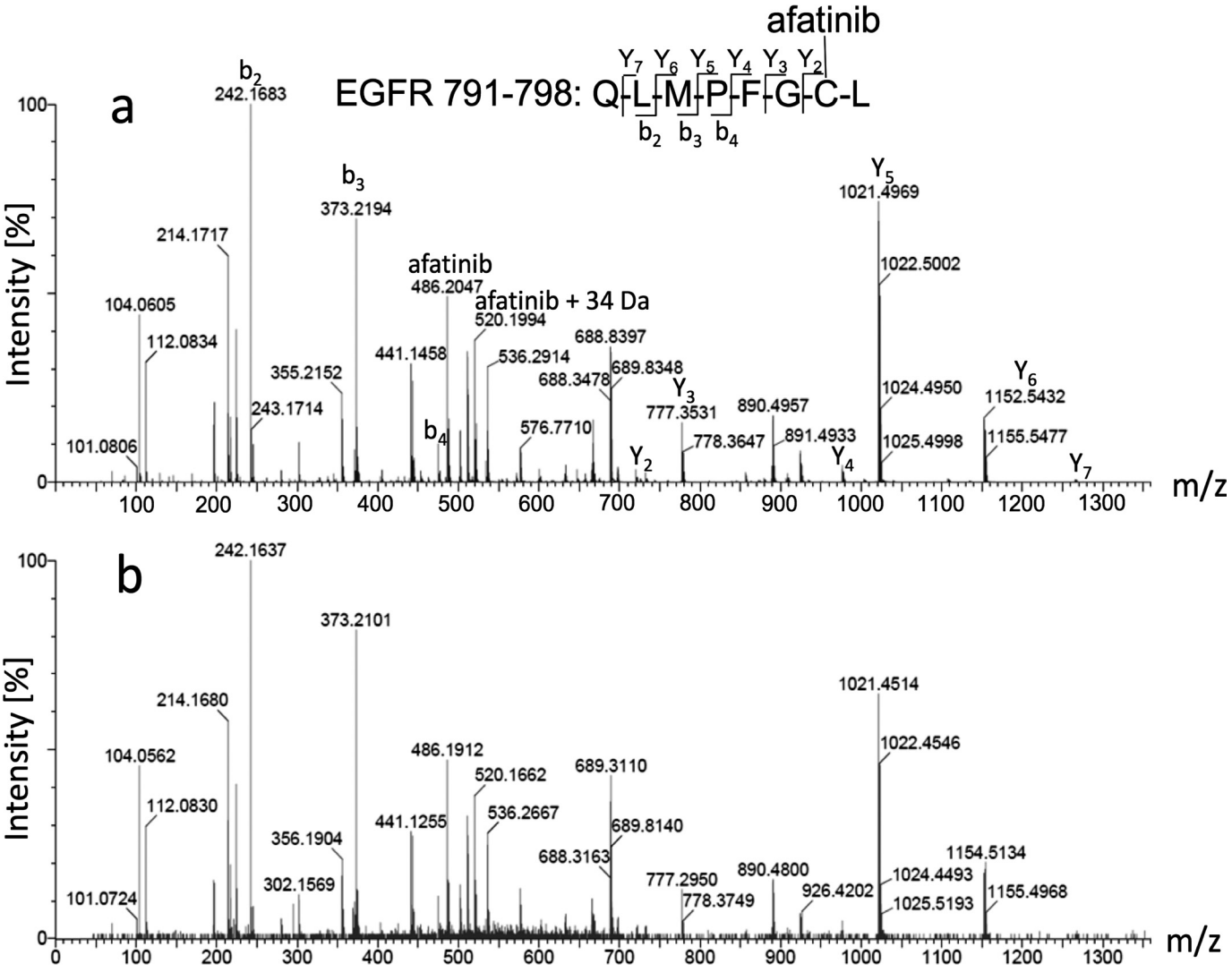

Fig. 4. Comparison of fragmentation mass spectra (MS/MS) demonstrates covalent binding of afatinib to $EGFR^{T790M/L858R}$. Chemically synthesized EGFR peptide amino acids 791–798, covalently modified with afatinib (A) and the corresponding peptide, isolated from the $EGFR^{T790M/L858R}$ kinase domain after incubation with afatinib (B) were resolved by liquid chromatography/tandem mass spectrometry. The peptide sequence was derived from information of *b*- and *y*-ion fragmentation series, isotopic distribution patterns of fragments, and the mass of the parent ion. Identified ions of the *b*- and *y*-ion fragmentation series have been annotated.

49 nM) or HER2 (BT474, 75 nM), BI 37781 did not potently inhibit signaling in these cell lines displaying EC_{50} values above 500 nM. The difference in inhibitory profile was confirmed in proliferation assays where afatinib displayed nanomolar activity (NCI-H1975, 92 nM; BT474, 54 nM), whereas BI 37781 was ineffective even at high concentrations (>4000 nM). In agreement with this observation, the irreversible inhibitor canertinib showed an inhibitory profile similar to afatinib, whereas the reversible inhibitors gefitinib and erlotinib showed activity similar to that of BI 37781 (Table 1). Because afatinib has been shown to interact with and inhibit ErbB-4 protein expression, ErbB-4 phosphorylation was determined after 2 h of incubation with kinase inhibitors in NIH3T3 mouse fibroblasts transfected with a plasmid encoding full-length ErbB-4 (Fig. 5A). Inhibition of constitutive ErbB-4 phosphorylation by afatinib started at 30 nM and was complete at 300 nM. Whereas the covalent inhibitor canertinib showed full inhibition at 1000 nM, the noncovalent inhibitors lapatinib, gefitinib, and erlotinib had no detectable effect on ErbB-4 phosphorylation at this concentration. Cellular washout experiments were performed to explore whether irreversible enzyme inhibition by covalently binding inhibitors results in prolonged duration of action. To this end, A431 cells expressing wild-type EGFR were incubated overnight in serum-free media to induce receptor dephosphorylation. Pretreatment with reversible and irreversible ErbB inhibitors at 300 nM for 1 h prevented EGF-induced EGFR activation in all cases (Fig. 5B). When the cells were washed after exposure to the inhibitors and incubated for 8 h before the addition of EGF, receptor phosphorylation was observed only in cells pretreated with reversible inhibitors (BI 37781 and gefitinib), whereas activation was prevented in cells treated with irreversible inhibitors (afatinib and canertinib). A lag time of 24 to 48 h was necessary for these cells to regain full sensitivity to EGF stimulation, which is in line with the kinetics of de novo EGFR biosynthesis in this cell line (Decker 1984). These results suggest that covalent EGFR inhibitors might have advantages compared with reversible inhibitors because of their long-lasting inhibition of receptor phosphorylation.

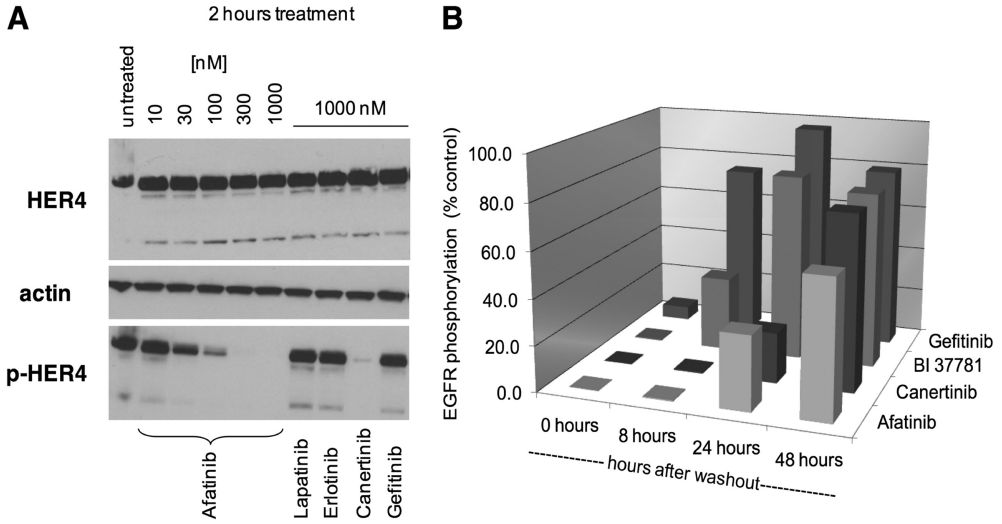

Fig. 5. Cellular experiments confirm ErbB-4 inhibition and prolonged duration of action of afatinib on EGFR. A, NIH3T3 cells transiently transfected with an ErbB-4 expression vector (48 h) were incubated with kinase inhibitors for 2 h before lysis. The resulting extracts (50 μg per lane) were resolved by SDS-polyacrylamide gel electrophoresis, transferred to polyvinylidene difluoride membranes, and probed with the rabbit monoclonal antibodies 83B10 (HER4) and 21A9 (phosphorylated ErbB-4; Tyr1284). B, A431 cells were incubated with inhibitors at a final concentration of 300 nM in serum-free media for 1 h before stimulation with 100 ng/ml EGF. The bars in the graph (mean of six replicates) represent the EGFR phosphorylation status at different time points after drug washout.

Discussion

Inhibition of aberrant ErbB receptor signaling has been at the forefront of personalized medicine in various indications including breast, colon, lung, and stomach cancer. Targeted drugs including monoclonal antibodies (cetuximab, panitumumab, and trastuzumab) and ATP-competitive kinase inhibitors (gefitinib, erlotinib, and lapatinib) have been approved by health authorities. Newer chemical entities targeting ErbB receptors were designed to covalently engage their targets characterized by cysteine residues in the active site, assuming that this might translate into higher selectivity and longer residence time and, ultimately, into better efficacy (Copeland et al., 2006; Singh et al., 2011). The initial synthetic work by Fry et al. (1994) on EGFR inhibitors paved the way for the development of such compounds. We have conducted a chemical synthesis program aiming for the discovery of irreversible inhibitors targeting all enzymatically active ErbB receptors in homodimeric and heterodimeric complexes, reasoning that drugs displaying a profile such as afatinib would provide an effective, long-lasting blockade of aberrant ErbB receptor signaling in multiple types of cancer. To more closely examine the role of irreversible target binding, we have synthesized a tool compound, BI 37781, which is almost identical in structure to afatinib except that the reactive double bond required for covalent binding to cysteine residues was replaced by a single bond.

Using SPR analysis as a biophysical approach to characterize drug-target interactions we observed that at pH 7.0 the sensorgrams of wild-type EGFR exposed to afatinib or BI 37781 were very similar. In contrast, afatinib dissociated more slowly than its analog from mutant $EGFR^{L858RT790M}$. Additional interaction analyses showed that at conditions favoring covalent bond formation (pH 8) afatinib dissociated more slowly from both wild-type and mutant targets than BI 37781, a result in line with covalent bond formation. X-ray crystallography of afatinib in complex with the kinase domain of wild-type EGFR unequivocally proved the formation of a covalent bond to Cys797 and also revealed that afatinib binds to the kinase in its active conformation. This binding mode contrasts with the one of lapatinib, which reportedly requires the inactive conformation to accommodate the larger aromatic group attached to the aniline (Wood et al., 2004). The crystal structure of the $EGFR^{T790M}$ variant in complex with afatinib hinted toward covalent binding (Protein Data Bank ID code 4G5P), and the binding mode was further investigated by using mass spectrometry. Using this approach we could demonstrate the ability of afatinib to chemically react and form a covalent bond under physiological conditions (pH 7.5; 37°C) with EGFR, $EGFR^{L858R/T790M}$, HER2, and ErbB-4. However, because it had been reported that some types of covalent binding, such as Michael addition can be reversible (Lin et al., 2008), we wanted to show that covalent binding is also relevant in cancer cells. To this end, we investigated functional differences between afatinib and its analog BI 37781 in biological systems and included additional, well described tyrosine kinase inhibitors for comparison, including compounds capable of covalent binding (canertinib) and others (erlotinib, gefitinib, and lapatinib), which, like BI 37781, lack chemical reactivity. We observed that inhibition of proliferation of $EGFR^{L858R/T790M}$-containing lung cancer cells seems to require the presence of the Michael acceptor group (EC_{50} afatinib and canertinib, 0.1 μM; all other compounds, >4 μM). Because clonal emergence of $EGFR^{T790M}$ mutations is the cause of drug resistance in approximately 50% of patients with non–small-cell lung cancer relapsing on erlotinib or gefitinib treatment, these differences in potency may be of clinical relevance. In comparison with afatinib or canertinib, BI 37781, erlotinib, and gefitinib were much less potent inhibitors of BT474 breast cancer cell proliferation that is known to be driven by overexpressed HER2. Lapatinib, in contrast, was almost as potent as the covalent binders, indicating that covalent target interaction is not essential for effective HER2 kinase inhibition. Afatinib was also identified as a potent inhibitor of ErbB-4 activity in cellular assays. Constitutive ErbB-4 phosphorylation in transfected NIH3T3 cells was blocked by afatinib and canertinib, but not by reversible inhibitors. Finally, we observed that the presence of the Michael acceptor group also resulted in prolonged duration of EGFR inhibition in cellular washout experiments. Signaling, as determined by measuring EGF-induced EGFR phosphorylation, was restored at least partially within 8 h and to full extent within 24 h of removal of reversible EGFR binders. In contrast, restoration of kinase activity required up to 48 h after washout of irreversible

inhibitors, consistent with the hypothesis that kinase activity can be restored only by de novo biosynthesis of the receptor proteins. These results provide circumstantial evidence for a covalent bond formation in these cells and point to possible pharmacodynamic advantages of irreversibly binding inhibitors, which could provide persistent target inhibition in vivo even after clearance of the drug from the system.

The plasticity of the ErbB network has recently been implicated in resistance to ErbB targeting agents such as cetuximab (Vlacich and Coffey, 2011) or trastuzumab (Narayan et al., 2009). De novo or acquired resistance to cetuximab can develop through receptor mutations (S492R; Montagut et al., 2012), ErbB2 amplification and increased heregulin synthesis (Yonesaka et al., 2011), or generation of HER2 isoforms by alternative splicing (e.g., 611-CTF; Quesnelle and Grandis, 2011). Likewise, resistance to trastuzumab in breast carcinoma cells may be mediated by increased expression of EGFR and ErbB-3 (Narayan et al., 2009) and cognate ErbB ligands (Ritter et al., 2007) or truncated HER2 isoforms such as p95HER2 (Scaltriti et al., 2007). Our results indicate that afatinib is able to effectively silence aberrant ErbB network activity emanating from all homotypic and heterotypic dimers formed; when used as a single agent or in drug combinations, afatinib thus may delay or prevent emergence of resistance caused by ErbB reprogramming. Ongoing late-stage clinical trials evaluating the efficacy and safety of afatinib in patients with cancers of the head and neck, lung (mutant EGFR), and breast (amplified HER2) ultimately will reveal whether the distinct pharmacological features of this compound translate into improved patient benefit.

Acknowledgments

We thank the staff at Beactica AB, Uppsala, Sweden for performing the SPR experiments; all present and past members of the Afatinib research and development teams and their collaborators for excellent technical contributions; and Dr. Jürgen Moll for diligent and critical reviewing.

Authorship Contributions

Participated in research design: Solca, Dahl, Zoephel, Bader, Sanderson, Klein, Kraemer, and Haaksma.

Conducted experiments: Solca and Zoephel.

Contributed new reagents or analytic tools: Himmelsbach.

Performed data analysis: Solca, Dahl, Zoephel, Bader, Sanderson, and Adolf.

Wrote or contributed to the writing of the manuscript: Solca, Dahl, Zoephel, Bader, and Adolf.

References

Alvarado D, Klein DE, and Lemmon MA (2009) ErbB2 resembles an autoinhibited invertebrate epidermal growth factor receptor. *Nature* **461:**287–291.

Bang YJ, Van Cutsem E, Feyereislova A, Chung HC, Shen L, Sawaki A, Lordick F, Ohtsu A, Omuro Y, Satoh T, et al. (2010) Trastuzumab in combination with chemotherapy versus chemotherapy alone for treatment of HER2-positive advanced gastric or gastro-oesophageal junction cancer (ToGA): a phase 3, open-label, randomised controlled trial. *Lancet* **376:**687–697.

Collaborative Computational Project, Number 4 (1994) The CCP4 suite: programs for protein crystallography. *Acta Crystallogr D Biol Crystallogr* **50:**760–763.

Copeland RA, Pompliano DL, and Meek TD (2006) Drug-target residence time and its implications for lead optimization. *Nat Rev Drug Discov* **5:**730–739.

Decker SJ (1984) Aspects of the metabolism of the epidermal growth factor receptor in A431 human epidermoid carcinoma cells. *Mol Cell Biol* **4:**571–575.

Dengler WA, Schulte J, Berger DP, Mertelsmann R, and Fiebig HH (1995) Development of a propidium iodide fluorescence assay for proliferation and cytotoxicity assays. *Anticancer Drugs* **6:**522–532.

Eck MJ and Yun CH (2010) Structural and mechanistic underpinnings of the differential drug sensitivity of EGFR mutations in non-small cell lung cancer. *Biochim Biophys Acta* **1804:**559–566.

Emsley P, Lohkamp B, Scott WG, and Cowtan K (2010) Features and development of Coot. *Acta Crystallogr D Biol Crystallogr* **66:**486–501.

Fry DW, Kraker AJ, McMichael A, Ambroso LA, Nelson JM, Leopold WR, Connors RW, and Bridges AJ (1994) A specific inhibitor of the epidermal growth factor receptor tyrosine kinase. *Science* **265:**1093–1095.

Garrett TP, McKern NM, Lou M, Elleman TC, Adams TE, Lovrecz GO, Kofler M, Jorissen RN, Nice EC, Burgess AW, et al. (2003) The crystal structure of a truncated ErbB2 ectodomain reveals an active conformation, poised to interact with other ErbB receptors. *Mol Cell* **11:**495–505.

Graus-Porta D, Beerli RR, Daly JM, and Hynes NE (1997) ErbB-2, the preferred heterodimerization partner of all ErbB receptors, is a mediator of lateral signaling. *EMBO J* **16:**1647–1655.

Ji H, Zhao X, Yuza Y, Shimamura T, Li D, Protopopov A, Jung BL, McNamara K, Xia H, Glatt KA, et al. (2006) Epidermal growth factor receptor variant III mutations in lung tumorigenesis and sensitivity to tyrosine kinase inhibitors. *Proc Natl Acad Sci U S A* **103:**7817–7822.

Kabsch W (2010) Integration, scaling, space-group assignment and post-refinement. *Acta Crystallogr D Biol Crystallogr* **66:**133–144.

Li D, Ambrogio L, Shimamura T, Kubo S, Takahashi M, Chirieac LR, Padera RF, Shapiro GI, Baum A, Himmelsbach F, et al. (2008) BIBW2992, an irreversible EGFR/HER2 inhibitor highly effective in preclinical lung cancer models. *Oncogene* **27:**4702–4711.

Lin D, Saleh S, and Liebler DC (2008) Reversibility of covalent electrophile-protein adducts and chemical toxicity. *Chem Res Toxicol* **21:**2361–2369.

Lynch TJ, Bell DW, Sordella R, Gurubhagavatula S, Okimoto RA, Brannigan BW, Harris PL, Haserlat SM, Supko JG, Haluska FG, et al. (2004) Activating mutations in the epidermal growth factor receptor underlying responsiveness of non-small-cell lung cancer to gefitinib. *N Engl J Med* **350:**2129–2139.

Montagut C, Dalmases A, Bellosillo B, Crespo M, Pairet S, Iglesias M, Salido M, Gallen M, Marsters S, Tsai SP, et al. (2012) Identification of a mutation in the extracellular domain of the epidermal growth factor receptor conferring cetuximab resistance in colorectal cancer. *Nat Med* **18:**221–223.

Narayan M, Wilken JA, Harris LN, Baron AT, Kimbler KD, and Maihle NJ (2009) Trastuzumab-induced HER reprogramming in "resistant" breast carcinoma cells. *Cancer Res* **69:**2191–2194.

Oberth CA and Jones AD (1997) Fragmentation of protonated thioether conjugates of acrolein using low collision energies. *J Am Soc Mass Spectrom* **8:**727–736.

Prickett TD, Agrawal NS, Wei X, Yates KE, Lin JC, Wunderlich JR, Cronin JC, Cruz P, Rosenberg SA, and Samuels Y (2009) Analysis of the tyrosine kinome in melanoma reveals recurrent mutations in ERBB4. *Nat Genet* **41:**1127–1132.

Quesnelle KM and Grandis JR (2011) Dual kinase inhibition of EGFR and HER2 overcomes resistance to cetuximab in a novel in vivo model of acquired cetuximab resistance. *Clin Cancer Res* **17:**5935–5944.

Ritter CA, Perez-Torres M, Rinehart C, Guix M, Dugger T, Engelman JA, and Arteaga CL (2007) Human breast cancer cells selected for resistance to trastuzumab in vivo overexpress epidermal growth factor receptor and ErbB ligands and remain dependent on the ErbB receptor network. *Clin Cancer Res* **13:**4909–4919.

Scaltriti M, Rojo F, Ocaña A, Anido J, Guzman M, Cortes J, Di Cosimo S, Matias-Guiu X, Ramon y Cajal S, Arribas J, et al. (2007) Expression of p95HER2, a truncated form of the HER2 receptor, and response to anti-HER2 therapies in breast cancer. *J Natl Cancer Inst* **99:**628–638.

Singh J, Petter RC, Baillie TA, and Whitty A (2011) The resurgence of covalent drugs. *Nat Rev Drug Discov* **10:**307–317.

Slamon DJ, Clark GM, Wong SG, Levin WJ, Ullrich A, and McGuire WL (1987) Human breast cancer: correlation of relapse and survival with amplification of the HER-2/neu oncogene. *Science* **235:**177–182.

Sleno L, Varesio E, and Hopfgartner G (2007) Determining protein adducts of fipexide: mass spectrometry based assay for confirming the involvement of its reactive metabolite in covalent binding. *Rapid Commun Mass Spectrom* **21:**4149–4157.

Solca FF, Baum A, Langkopf E, Dahmann G, Heider KH, Himmelsbach F, and van Meel JC (2004) Inhibition of epidermal growth factor receptor activity by two pyrimidopyrimidine derivatives. *J Pharmacol Exp Ther* **311:**502–509.

Stamos J, Sliwkowski MX, and Eigenbrot C (2002) Structure of the epidermal growth factor receptor kinase domain alone and in complex with a 4-anilinoquinazoline inhibitor. *J Biol Chem* **277:**46265–46272.

Tzahar E, Waterman H, Chen X, Levkowitz G, Karunagaran D, Lavi S, Ratzkin BJ, and Yarden Y (1996) A hierarchical network of interreceptor interactions determines signal transduction by Neu differentiation factor/neuregulin and epidermal growth factor. *Mol Cell Biol* **16:**5276–5287.

Vlacich G and Coffey RJ (2011) Resistance to EGFR-targeted therapy: a family affair. *Cancer Cell* **20:**423–425.

Wood ER, Truesdale AT, McDonald OB, Yuan D, Hassell A, Dickerson SH, Ellis B, Pennisi C, Horne E, Lackey K, et al. (2004) A unique structure for epidermal growth factor receptor bound to GW572016 (Lapatinib): relationships among protein conformation, inhibitor off-rate, and receptor activity in tumor cells. *Cancer Res* **64:**6652–6659.

Yarden Y and Sliwkowski MX (2001) Untangling the ErbB signalling network. *Nat Rev Mol Cell Biol* **2:**127–137.

Yonesaka K, Zejnullahu K, Okamoto I, Satoh T, Cappuzzo F, Souglakos J, Ercan D, Rogers A, Roncalli M, Takeda M, et al. (2011) Activation of ERBB2 signaling causes resistance to the EGFR-directed therapeutic antibody cetuximab. *Sci Transl Med* **3:**99ra86.

Yun CH, Mengwasser KE, Toms AV, Woo MS, Greulich H, Wong KK, Meyerson M, and Eck MJ (2008) The T790M mutation in EGFR kinase causes drug resistance by increasing the affinity for ATP. *Proc Natl Acad Sci U S A* **105:**2070–2075.

Zhang H, Berezov A, Wang Q, Zhang G, Drebin J, Murali R, and Greene MI (2007) ErbB receptors: from oncogenes to targeted cancer therapies. *J Clin Invest* **117:**2051–2058.

Zhang X, Gureasko J, Shen K, Cole PA, and Kuriyan J (2006) An allosteric mechanism for activation of the kinase domain of epidermal growth factor receptor. *Cell* **125:**1137–1149.

Address correspondence to: Flavio Solca, Doktor-Böhringer-Gasse 5-11, A-1120, Vienna, Austria, E-mail: flavio.solca@boehringer-ingelheim.com